Figure 3 Difference in maximum organism sizes between Maastrichtian and Danian sister taxa.

nutrient stress throughout much of the year[13,14]. Furthermore, the proportion of phytodetritus reaching the sea floor rapidly decreases below the euphotic zone[14]. The observed pattern could, therefore, have been produced by a decrease in phytoplankton abundance at the end of the Cretaceous that was not so large as seriously to affect plankotrophic larvae living and feeding in the euphotic zone, but which reduced the organic matter reaching the sea floor sufficiently to trigger widespread extinction of already nutrient-stressed deposit feeders.

It is possible that the final blow was dealt by asteroid impact, but there is indirect evidence that conditions for plankton were becoming less favourable immediately before the K/T boundary. Climate was rapidly deteriorating[15] and extinction of several major molluscan groups had already taken place[16]. Furthermore, numerous lineages of echinoids independently switched to non-planktotrophic development in the Maastrichtian, regardless of palaeolatitude and water depth[17], implying that survival for planktonic feeding larvae was becoming markedly less predictable. Furthermore, the fact that high levels of extinction continued into the Danian suggests a slow squeeze rather than an instantaneous catastrophe.

Finally, we note a dramatic decrease in size of post-Cretaceous survivors. Almost all Danian echinoids are significantly smaller than their Maastrichtian antecedents (Fig. 3) and apparently remained so until the latter half of the Danian. Early Danian echinoids either grew much more slowly or became more opportunistic, achieving sexual maturity at a much earlier stage. In either case, the small size of Danian survivors is consistent with nutrient supply remaining unpredictable and a limiting factor to growth for a considerable time interval following the K/T event, as postulated previously[18]. □

1. Jablonski, D. Mass extinctions: persistent problems and new directions. *Geol. Soc. Am. Spec. Pap.* **307**, 1–9 (1996).
2. Jablonski, D. in *Dynamics of Extinction* (ed. Elliott, D. K.) 183–229 (Wiley, New York, 1986).
3. Jablonski, D. & Raup, D. M. Selectivity of end-Cretaceous marine bivalve extinction. *Science* **268**, 389–391 (1995).
4. Jablonski, D. Progress at the K–T boundary. *Nature* **387**, 354–355 (1997).
5. Smith, A. B. & Jeffery, C. H. Fossil echinoids of the Maastrichtian and Palaeocene: an illustrated key. *Spec. Pap. Palaeont.* (submitted).
6. Sheehan, P. M., Coorough, P. J. & Fastovsky, D. E. Biotic selectivity during the K/T and late Ordovician extinction events. *Geol. Soc. Am. Spec. Pap.* **307**, 477–489 (1996).
7. Johansen, M. B. Background extinction and mass extinction of the brachiopods from the chalk of northwest Europe. *Palaios* **4**, 243–250 (1989).
8. De Ridder, C. & Lawrence, J. M. in *Echinoderm Nutrition* (eds Jangoux, M. & Lawrence, J. M.) (Balkema, Rotterdam, 1982).
9. Smith, A. B. The structure, function and evolution of tube feet and ambulacral pores in irregular echinoids. *Palaeontology* **23**, 39–83 (1980).
10. Telford, M. & Mooi, R. Podial particle picking in *Cassidulus caribaearum* (Echinodermata: Echinoidea) and the phylogeny of sea urchin feeding mechanism. *Biol. Bull.* **191**, 209–223 (1996).
11. Rose, E. P. F. Some observations on the recent holectypoid echinoid *Echinoneus cyclostomus* and their palaeoecological significance. *Thalass. Jugoslav.* **12**, 299–306 (1978).
12. Valentine, J. W. & Jablonski, D. Mass extinctions: sensitivity of marine larval types. *Proc. Natl Acad. Sci. USA* **83**, 6912–6914 (1986).
13. Levinton, J. S. Trophic group and the end-Cretaceous extinction: did deposit feeders have it made in the shade? *Paleobiology* **22**, 104–112 (1996).
14. Summerhayes, C. P. & Thorpe, S. A. *Oceanography, an Illustrated Guide* (Manson, London, 1996).
15. Barrera, E. Global environmental change preceding the Cretaceous–Tertiary boundary: Early–late Maastrichtian transition. *Geology* **22**, 877–880 (1994).
16. Macleod, N. *et al.* The Cretaceous–Tertiary biotic transition. *J. Geol. Soc. Lond.* **154**, 265–292 (1997).
17. Jeffery, C. H. Dawn of echinoid nonplanktotrophy: coordinated shifts in development indicate environmental instability prior to the K–T boundary. *Geology* **25**, 991–994 (1997).
18. D'Hondt, S., Herbert, T. D., King, J. & Gibson, C. Planktonic foraminifera, asteroids, and marine production: death and recovery at the Cretaceous–Tertiary boundary. *Geol. Soc. Am. Spec. Pap.* **307**, 303–317 (1996).

A molecular evolutionary framework for the phylum Nematoda

Mark L. Blaxter*, **Paul De Ley**†‡, **James R. Garey**§,
Leo X. Liu‖¶, **Patsy Scheldeman**†, **Andy Vierstraete**†,
Jacques R. Vanfleteren†, **Laura Y. Mackey**#, **Mark Dorris***,
Linda M. Frisse☆, **J. T. Vida**☆ **& W. Kelley Thomas**☆

* *Institute of Cell, Animal and Population Biology, King's Buildings, University of Edinburgh, Edinburgh EH9 3JT, UK*
† *Department of Morphology, Systematics and Ecology, University of Gent, B-9000 Gent, Belgium*
‡ *International Institute of Parasitology, St Albans AL4 0XU, UK*
§ *Department of Biological Sciences, University of South Florida, Tampa, Florida 33620, USA*
‖ *Harvard-Thorndike Laboratory, Department of Medicine, Beth Israel Deaconess Medical Center, Harvard Medical School, Boston, Massachusetts 02215, USA*
¶ *NemaPharm, Inc, 26 Landsdowne Street, Cambridge, Massachusetts 02139, USA*
# *Department of Molecular Physiology and Biophysics, Baylor College of Medicine, Houston, Texas 77030, USA*
☆ *Division of Molecular Biology and Biochemistry, School of Biological Sciences, University of Missouri, Kansas City, Missouri 64110, USA*

Nematodes are important: parasitic nematodes threaten the health of plants, animals and humans on a global scale[1,2]; interstitial nematodes pervade sediment and soil ecosystems in overwhelming numbers[3]; and *Caenorhabditis elegans* is a favourite experimental model system[4]. A lack of clearly homologous characters and the absence of an informative fossil record have prevented us from deriving a consistent evolutionary framework for the phylum. Here we present a phylogenetic analysis, using 53 small subunit ribosomal DNA sequences from a wide range of nematodes. With this analysis, we can compare animal-parasitic, plant-parasitic and free-living taxa using a common measurement. Our results indicate that convergent morphological evolution may be extensive and that present higher-level classification of the Nematoda will need revision. We identify five major clades within the phylum, all of which include parasitic species. We suggest that animal parasitism arose independently at least four times, and plant parasitism three times. We clarify the relationship of *C. elegans* to major parasitic groups; this will allow more effective exploitation of our genetic and biological knowledge of this model species.

To study the evolutionary relationships within the phylum, we constructed a database of small subunit (SSU) sequences from 53 taxa, including 41 new sequences[5-9]. Species were chosen to cover all the major parasitic and free-living taxonomic groups. Sequences were aligned with reference to a secondary-structure model[5] and on the basis of similarity[8]. Model phylogenies were evaluated under the criteria of maximum parsimony (MP), maximum likelihood (ML)

and minimum evolution using the neighbour-joining (NJ) method[10], and were tested for statistical support with careful consideration of unequal rate effects[11]. The consensus of the shortest MP trees found is shown in Fig. 1. The overall consensus of our analyses is shown in Fig. 2a and can be compared with a representation of previous hypotheses, shown in Fig. 2b. Our hypothesis is based on a study of a single genetic locus but permits, for the first time, the comparison of all taxa using the same defined measurement.

Nematoda is traditionally divided into two classes, namely, the predominantly terrestrial Secernentea and the predominantly marine Adenophorea. Contrary to this view, our analyses indicate

that the Adenophorea may be paraphyletic, as it includes the ancestors of the Secernentea. Phylogenies in which the Adenophorea is monophyletic by outgroup rooting score significantly worse in all methods of analysis. This result is supported by some morphological analyses which indicate the lack of synapomorphies (common characters) for Adenophorea[12] or place Secernentea as a monophyletic clade derived from adenophorean ancestry[13]. Two purely adenophorean clades are strongly supported (clades I and II in Fig. 2). Clade I groups the vertebrate-parasitic order Trichocephalida with the insect-parasitic Mermithida, plant-parasitic Dorylaimida and free-living Mononchida. Clade II links the plant-parasitic Triplonchida with the free-living Enoplida. Our analyses do not place the orders
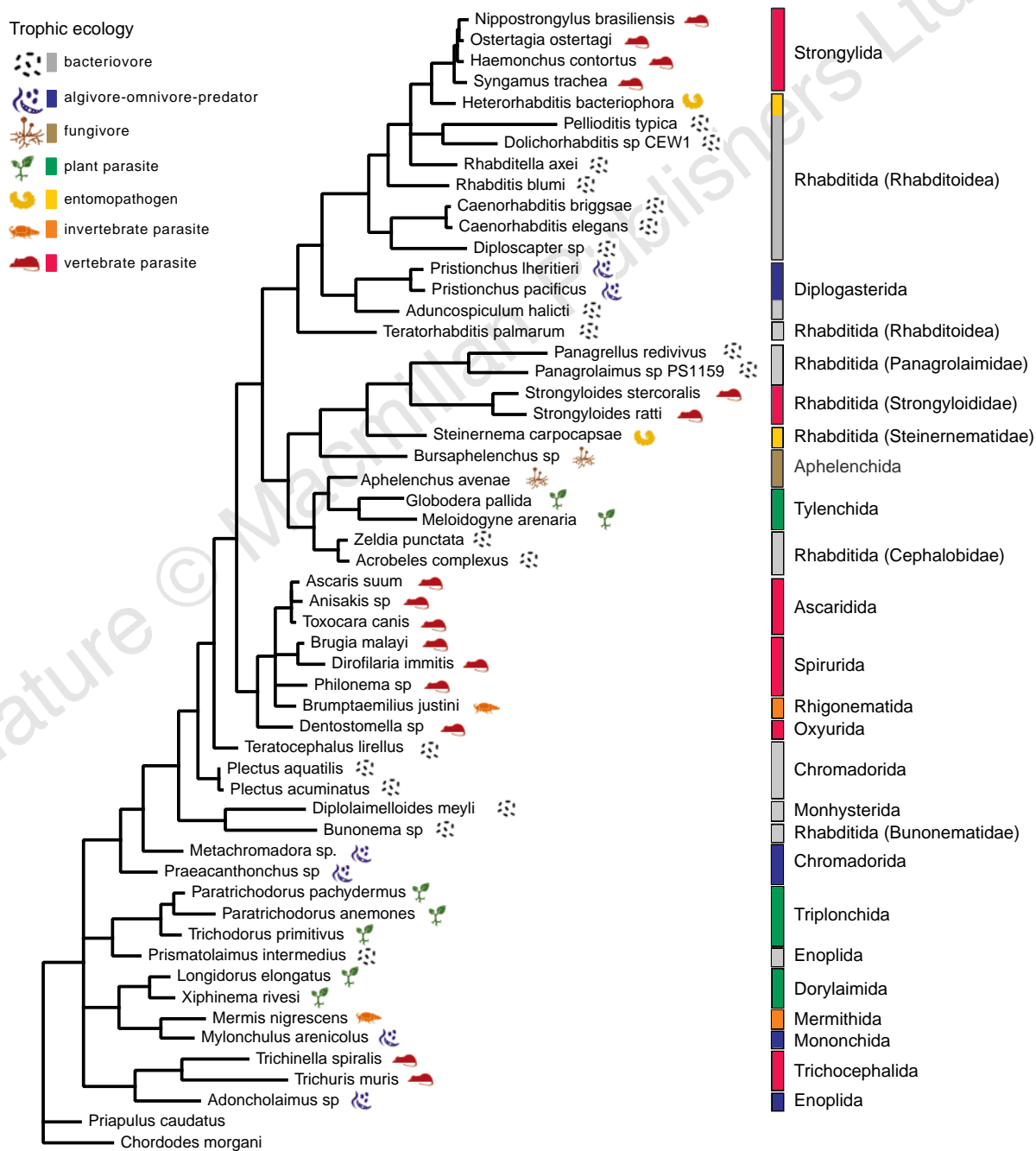

Figure 1 MP analysis of SSU sequences from 53 nematode taxa. Nearly complete SSU sequences (see Methods) were aligned and processed for MP analysis. Twenty-four shortest trees (requiring 3,583 nucleotide changes) were found; the tree presented is the strict consensus of these. Branch lengths are drawn to be proportional to the number of changes inferred. The trophic ecologies of the taxa are represented by coloured icons. No shorter trees were revealed by local searching of subsets of the data[24]. *Priapulus* (a priapulid) and *Chordodes* (a nematomorph) were defined as outgroups[11,21]. In this tree, as with all MP trees constructed with subsets of the data, *Plectus* is a sister taxon to the Secernentea (see Fig. 2).
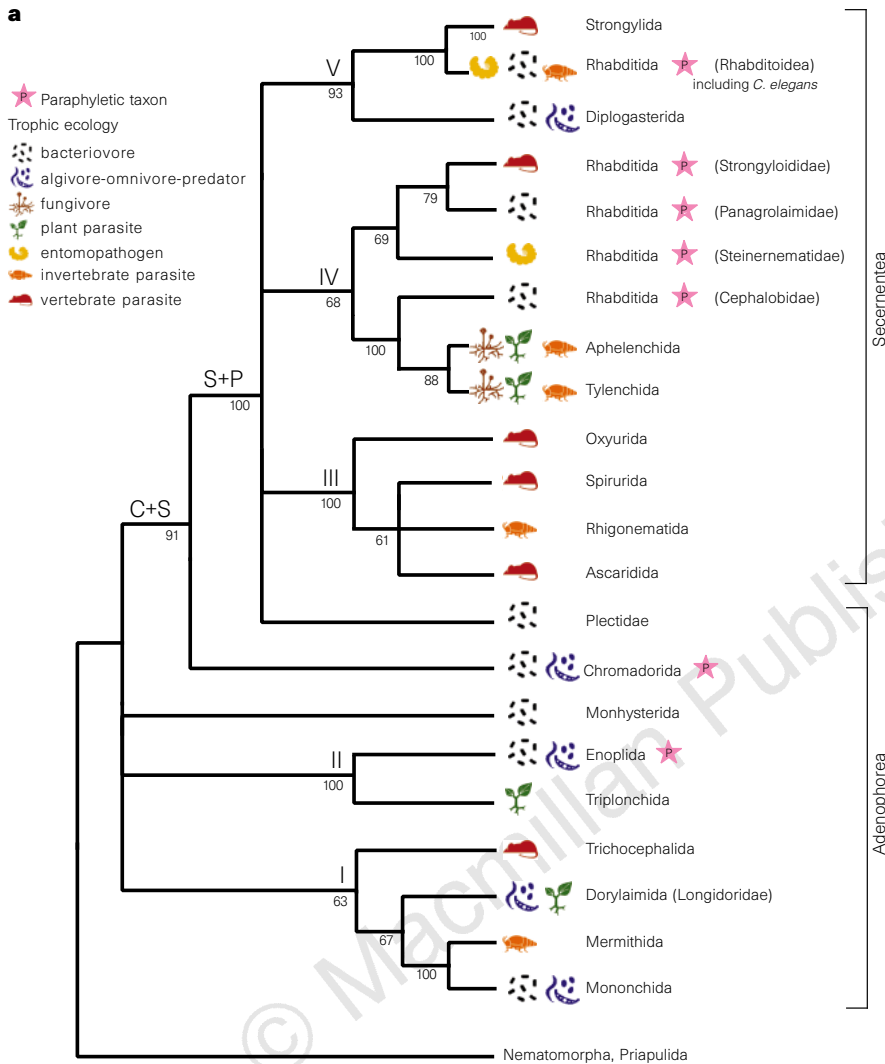
Figure 2 A phylogenetic hypothesis for the phylum Nematoda based on the SSU-sequence dataset. **a**, A dendrogram summarizing the results of our MP and NJ analyses. For each branchpoint, the maximal percentage bootstrap support in NJ analyses is given. We define five major clades in the Nematoda (from bottom, I–V). C + S indicates the clade Chromadorida plus Secernentea, and S + P indicates Secernentea plus Plectidae. Trophic ecologies are indicated as in Fig. 1. Currently accepted taxa that we find to be paraphyletic are indicated with a starred P. **b**, Our interpretation of the currently accepted systematics of the orders and genera considered in this study, represented as a cladogram and derived from several sources[2,12–14].
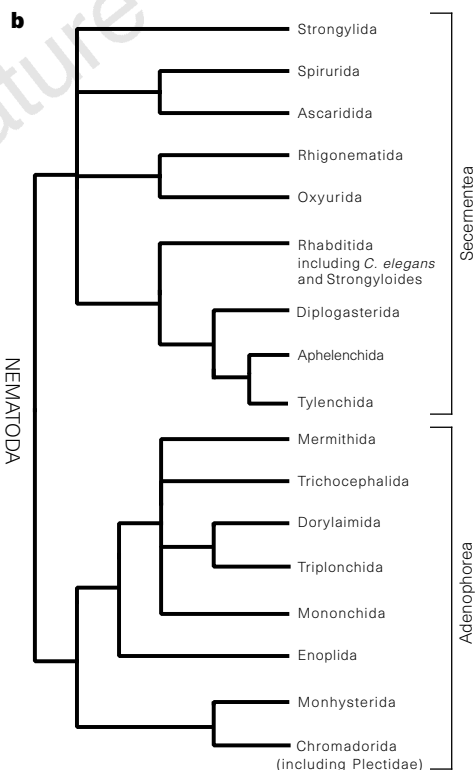
Triplonchida and Dorylaimida as sister taxa, in contrast to the results of previous studies[12–14]. The single sampled representative of the order Monhysterida does not given an unequivocal position for this group.

The Chromadorida are a large and diverse group of mostly microbivorous nematodes, which have been proposed to include the ancestors of the terrestrial Secernentea[13]. The SSU data do not resolve the chromadorids as a distinct clade, but show a paraphyletic, comblike series of taxa at the base of the Secernentea. One chromadorid group, the Plectidae, is significantly associated with the secernentean clades (clade S + P of Fig. 2), suggesting that it may be a surviving representative of the group from within which the secernentean radiation began.

Most taxonomies divide the Secernentea into nine orders, with five of these including exclusively animal-parasitic taxa. We identify three major clades within the Secernentea (clades III, IV and V of Fig. 2); these clades do not correspond to the divisions of classical taxonomy. Instead, plant- and animal-parasitic orders are integrated within a radiation of free-living taxa. Clade III represents a novel grouping of vertebrate- and arthropod-parasitic taxa from the orders Ascaridida (large gut roundworms), Spirurida (filarial nematodes), Oxyurida (pinworms) and Rhigonematida (millipede-gut parasites). The order Rhabditida, a trophically diverse assemblage including some entomopathogenic and parasitic members, is paraphyletic, as 'rhabditid' taxa are found in two strongly supported clades, each of which includes a major parasitic order.

Clade IV (Fig. 2), a 'cephalobid' clade, groups the plant-parasitic orders Tylenchida (represented here by the cyst nematode genus *Globodera* and the root-knot nematode genus *Meloidogyne*) and Aphelenchida, the vertebrate-parasitic genus *Strongyloides* and the entomopathogenic genus *Steinernema* with free-living bacterio-vores of the rhabditid families Cephalobidae and Panagrolaimidae. The second clade (clade V of Fig. 2) groups *C. elegans* and other members of the suborder Rhabditina with the vertebrate-parasitic order Strongylida (small gut nematodes, including hookworms), the entomopathogenic genus *Heterorhabditis* and the order Diplogasterida. Diplogasterida, which includes *Pristionchus pacificus*, appears to be a sister group of some rhabidids, an observation supported by other molecular evidence[15]. *P. pacificus* has been proposed as a comparative model for *C. elegans*[16] and the relation-ship between these two taxa is now clear.

Although nematode parasites are generally assumed to have evolved from free-living ancestors, the precise origin and free-living sister taxa of each parasitic group are unknown. It has been suggested that all nematode parasites of animals are sufficiently closely related to be placed in the same subclass[12]. From our analysis we predict multiple origins for animal-parasitic taxa throughout the phylum. A minimum of four independent origins of vertebrate parasites is supported by bootstrap analysis (Fig. 2). In keeping with the view that vertebrate parasites evolved from arthropod-parasitic ancestors[2], each of the secernentean vertebrate-parasitic clades is associated with arthropod-parasitic or -pathogenic taxa (*Heterorhabditis* is associated with Strongylida; *Steinernema* is associated with Strongyloides; and Rhigonematida is associated with Ascaridida, Spirurida and Oxyurida). As there are extra vertebrate- and invertebrate-parasitic groups that have not yet been sampled in our analyses[2], the estimate of four independent origins is a minimum. Similarly, plant parasitism seems to have evolved independently three times in Nematoda, twice in the Adenophorea (the Dorylaimida and the Triplonchida) and once in the Secernentea (the Tylenchida).

Inconsistencies between this SSU phylogeny and earlier morpho-logical ones may partly arise because of convergent evolution. The genera *Steinernema* and *Heterorhabditis* share the unusual strategy of entomopathogenesis (after infecting insect hosts, the nematodes release toxic bacterial symbionts which quickly kill the host), but they do not share an exclusive common ancestry[17]. Similarly, some plant parasites in the orders Dorylaimida and Triplonchida transmit important plant viruses, yet these two orders are not closely related[18]. The pharynx of members of the orders Tylenchida and Aphelenchida resembles that of members of the free-living order Diplogasterida, suggesting a close relationship[19]. Our analysis places these two groups in different clades, suggesting two independent origins of this pharyngeal type.

Parasitic taxa are typically difficult to culture and analyse inde-pendently of their hosts. On the basis of our SSU data we can suggest free-living sister taxa that may act as good models for parasitic groups. Although *Strongyloides* is often thought to be related to rhabditids such as *C. elegans*[2], *Panagrellus* and its relatives may actually provide better comparative models for *Strongyloides* and *Steinernema*. *C. elegans* is, in fact, much more closely related to *Heterorhabditis* and vertebrate parasites of the order Strongylida than to any other parasitic clade, and should be a better model for these taxa. Similarly, the family Cephalobidae, which includes *Acrobeles* and *Zeldia*, could provide good models for the plant-parasitic Tylenchida. These affinities between free-living and para-sitic taxa are not apparent from existing classifications, although they do agree well with some morphological features (for example, the cellular structure of the posterior stoma region[20] and the occurrence of a male bursa with rays in Rhabditina–Strongylida, clade V). Our trees do not unequivocally indicate a closest free-living sister taxon for the compound animal-parasitic clade II. Plectidae is their sister taxon in some analyses, contrasting with the placement of *Plectus* basal to the Secernentea on the basis of multiple morphological characters[12].

It has been suggested that the SSU rDNA of *C. elegans* has evolved at a faster rate than usual in Metazoa[21]. Our dataset includes taxa with both fast (long branch length) and slow evolution rates. SSU sequences of the morphologically similar, free-living Rhabditida are highly divergent but the morphologically disparate, vertebrate-parasitic Strongylida show very little divergence. This indicates either that these groups have been classified previously at conflicting taxonomic levels, or that the parasitic groups have radiated rela-tively recently. The extent of sequence divergence between the vertebrate-parasitic taxa within clades III and V is of the same order as that of their hosts, but it is probably premature to apply host phylogenetic timing to the nematodes. Molecular phylogenetic inference can be used to provide an independent evolutionary framework with which to interpret nematode evolution. One of the most interesting implications of the SSU phylogeny is that parasitism has arisen many times from different free-living groups. By suggesting a relevant set of marker taxa, this evolutionary framework should lead to a structured approach to enable the exploitation of our knowledge of *C. elegans*. It will directly aid the investigation of the dynamics of morphological and developmental evolution[8,16] and the biology of parasitism. The generation of genome datasets from additional nematode species[22] will further aid this process. □

Methods

Isolation and sequencing of SSU genes. SSU genes were amplified by the polymerase chain reaction (PCR) from individual identified nematodes or from nematode DNA samples using universal SSU primers located close to the 5′ and 3′ ends. When possible, we determined the SSU sequence directly from the PCR product using a set of internal conserved primers which give complete coverage of both strands of the amplified fragment. When this approach did not yield satisfactory sequences, we sequenced cloned products from both strands. Several sequences were determined following an alternate protocol[8]. The sequences determined for this study are available in GenBank under the accession numbers U81506, U81574, U81575, U81579, U81581, U81582, AFO36586–AFO36612 and AFO36637–AFO36644. Details of material sources are available at http://www.ed.ac.uk/~mbx/nematode_ssu.html.

Alignment and phylogenetic analysis. We aligned the SSU sequences using a secondary-structure model[5]. The alignment contains 1,146 characters (exclud-ing gaps), of which 549 are informative for MP. Alternative alignments, including one in which any region involving an insertion or deletion was removed, gave nearly identical results, and did not change the deeper branching orders. The alignment was subjected to: MP analysis using PAUP v3.1.1 (ref. 23) and MacClade[24]; ML analysis of subsets and NJ analysis using gamma-corrected Kimura distances with MEGA v1.0 (ref. 25); and NJ analysis with gamma-corrected Kimura distances and substitution-rate compensation using Treecon v1.2 (refs 26, 27). Alpha values for gamma correction were estimated with PAML v1.2 (ref. 28) and Treecon v1.2; tree topology did not change signifi-cantly for alpha values between 0.3 and 1.0. To account for variable nucleotide composition between taxa, we performed log-determinant transformation of pairwise distances using test version 4.0d59 of PAUP*, written by D. L. Swofford. Constant sites were eliminated to minimize among-site rate hetero-geneity. NJ analysis of log-determinant-transformed data yielded a tree that was not significantly different from those produced by other NJ or MP analyses. We assessed statistical support using the bootstrap-resampling technique (200 bootstrap resamplings).

Rooting the tree. We used SSU sequences from a priapulid worm and a nematomorph as outgroup taxa; these represent the most closely related pseudocoelomate phyla[11]. A number of outgroup sequences from other pseudocoelomate phyla[21] was used with no effect on the internal structure of the trees. The placement of the root was supported in both MP and NJ trees. The only consistent difference between the two methods of analysis was in the placement of *Plectus*. In NJ analyses *Plectus* is the sister taxon to clade III of Fig. 2, with strong (>95%) bootstrap support. In MP analyses *Plectus* is placed basal to all Secernentea, but this position is not supported above 50% in

bootstrap replicates. ML analyses of these two trees showed that they are not significantly different.

Effects of long-branch taxa. To identify taxa with long apparent branch lengths, we performed a four-taxon NJ analysis (using gamma-corrected Kimura distances) using *Tripedalia* (a diploblast), *Antedon* (a deuterostome) and *Glycera* (a protostome) with each nematode taxon in turn. We recorded the inferred distance from the protostome–nematode node to the nematode taxon. MP distances were derived from the phylogeny presented in Fig. 1. These long-branch-length taxa often have extreme base-composition biases, but not all taxa with extreme base compositions have long branch lengths (for example, *Brugia* has an AT content of 79% but one of the shorter inferred branch lengths). NJ and MP analyses were re-performed with successive trimming of the long-branch taxa (distance >0.19 from root in four-taxon NJ analysis) from the dataset. As would be expected[29], exclusion of these taxa had effects on the bootstrap support for some clades. In particular, re-analysis excluding one or all of *Panagrellus*, *Panagrolaimus*, and *Strongyloides* yielded stronger bootstrap support for the cephalobid–steinernematid clade IV (<50% to 68%), and analyses excluding the long-branch rhabditid taxa *Bunonema*, *Teratorhabditis* and *Pellioditis* gave increased support for the Diplogasterida–Rhabditina clade V (51% to 93%). Figure 2a shows a consensus of these analyses: branchpoints that were supported by >60% in bootstrap long-branch taxa resampling of NJ or MP trees from the trimmed datasets were accepted. When there was no support for a resolved branching order, we collapsed nodes to form polytomies. Major clades supported by all analytical methods are shown and are numbered I–V. The association of Secernentea (clades II, IV and V) with the Plectidae has not been unequivocally resolved and is shown as a polytomy. We could not place the long-branch-length taxa in our trees with any certainty. We assessed statistical support for the placement of the vertebrate-parasitic taxa into four clades by calculating ML values for six-taxon subsets from the data. Each of the placements was strongly supported.

1. Luc, M., Sikora, R. A. & Bridge, J. *Plant Parasitic Nematodes in Tropical and Subtropical Agriculture* (CAB International, Wallingford, UK, 1990).
2. Anderson, R. C. *Nematode Parasites of Vertebrates. Their Development and Transmission* (CAB International, Wallingford, UK, 1992).
3. Lambshead, J. Recent developments in marine benthic biodiversity research. *Oceanis* **19**, 5–24 (1993).
4. Riddle, D., Blumenthal, T., Meyer, B. & Priess, J. (eds) *C. elegans II* (Cold Spring Harbor Laboratory Press, NY, 1997).
5. Ellis, R. E., Sulston, J. E. & Coulson, A. R. The rDNA of *C. elegans*: sequence and structure. *Nucleic Acids Res.* **14**, 2345–2364 (1986).
6. Zarlenga, D. S., Stringfellow, F., Nobary, M. & Lichtenfels, J. R. Cloning and characterisation of ribosomal RNA genes from three species of *Haemonchus* (Nematoda: Trichostrongyloidea) and identification of PCR primers for rapid differentiation. *Exp. Parasitol.* **78**, 28–36 (1994).
7. Fitch, D. H. A., Bugaj-gaweda, B. & Emmons, S. W. 18S ribosomal gene phylogeny for some rhabditidae related to *Caenorhabditis elegans*. *Mol. Biol. Evol.* **12**, 346–358 (1995).
8. Baldwin, J. G., Frisse, L. M., Vida, J. T., Eddleman, C. D. & Thomas, W. K. An evolutionary framework for the study of developmental evolution in a set of nematodes related to *Caenorhabditis elegans*. *Mol. Phylogenet. Evol.* **8**, 249–259 (1997).
9. Baldwin, J. G. *et al.* The buccal capsule of *Aduncospiculum halicti* (Nemata: Diplogasterina): an ultrastructural and molecular phylogenetic study. *Can. J. Zool.* **75**, 407–423 (1997).
10. Swofford, D. L., Olsen, G. J., Waddell, P. J. & Hillis, D. M. in *Molecular Systematics* (eds Hillis, D. M., Moritz, C. & Mable, B. K.) 407–514 (Sinauer, Sunderland, MA, 1996).
11. Aguinaldo, A. M. A. *et al.* Evidence for a clade of nematodes, arthropods and other moulting animals. *Nature* **387**, 489–493 (1997).
12. Lorenzen, S. *The Phylogenetic Systematics of Free-Living Nematodes* (The Ray Society, London, 1994).
13. Malakhov, V. V. *Nematodes. Structure, Development, Classification and Phylogeny* (Smithsonian Institution Press, Washington, 1994).
14. Maggenti, A. R. in *Concepts in Nematode Systematics* (eds Stone, A. R., Platt, H. M. & Khalil, L. F.) 25–40 (Academic, London, 1983).
15. Baldwin, J. G. & Eddleman, C. D. Buccal capsule of *Zeldia punctata* (Nemata: Cephalobidae): an ultrastructural study. *Can. J. Zool.* **73**, 648–656 (1995).
16. Etzinger, A. & Sommer, R. The homeotic gene *lin-39* and the evolution of nematode epidermal cell fates. *Science* **278**, 452–455 (1997).
17. Poinar, G. Origins and phylogenetic relationships of the entomophilic rhabditids, *Heterorhabditis* and *Steinernema*. *Fund. Appl. Nematol.* **16**, 332–338 (1993).
18. Siddiqi, M. R. Phylogenetic relationships of the soil orders Dorylaimida, Mononchida, Triplonchida and Alaimida, with a revised classification of the subclass Enoplia. *Pak. J. Nematol.* **1**, 79–110 (1983).
19. Poinar, G. O. *The Natural History of Nematodes* (Prentice-Hall, Englewood Cliffs, NJ, 1983).
20. De Ley, P., van de Velde, M. C., Mounport, D., Baujard, P. & Coomans, A. Ultrastructure of the stoma in Cephalobidae, Panagrolaimidae and Rhabditidae, with a proposal for a revised stoma terminology in Rhabditida. *Nematologica* **41**, 153–182 (1995).
21. Winnepenninckx, B. *et al.* 18S rRNA data indicate that Aschelminthes are polyphyletic in origin and consist of at least three distinct clades. *Mol. Biol. Evol.* **12**, 1132–1137 (1995).
22. Blaxter, M. L. *et al.* Genes expressed in *Brugia malayi* infective third stage larvae. *Mol. Biochem. Parasitol.* **77**, 77–96 (1996).
23. Swofford, D. L. *PAUP: Phylogenetic Analysis Using Parsimony, Version 3.1* (Illinois Natural History Society, Champaign, 1993).
24. Maddison, W. & Maddison, D. *MacClade v3.0* (Sinauer, Sunderland, MA, 1993).
25. Kumar, S., Tamura, K. & Nei, M. *MEGA: Molecular Evolutionary Genetics Analysis. Version 1.0* (Pennsylvania State Univ., 1993).
26. Van de Peer, Y., Rensing, S., Maire, U.-G. & De Wachter, R. Substitution rate calibration of small subunit subunit RNA identifies chlorarachniophyte nucleomorphs as remnants of green algae. *Proc. Natl Acad. Sci. USA* **93**, 7732–7736 (1996).
27. Van de Peer, Y. & De Wachter, R. TREECON for Windows: a software package for the construction and drawing of evolutionary trees for the Microsoft Windows environment. *Comput. Appl. Biosci.* **10**, 569–570 (1994).
28. Yang, Z. *Phylogenetic Analysis by Maximum Likelihood (PAML) Version 1.2* (Univ. California, Berkeley, 1996).
29. Felsenstein, J. Cases in which parsimony and compatibility methods will be positively misleading. *Syst. Zool.* **27**, 401–410 (1978).

Spatial and temporal organization during cardiac fibrillation

Richard A. Gray*†, **Arkady M. Pertsov*** & **José Jalife***

* *Department of Pharmacology, SUNY Health Science Center, 766 Irving Avenue, Syracuse, New York 13210, USA*
† *Department of Biomedical Engineering and Department of Medicine Division of Cardiovascular Disease, University of Albama at Birmingham, 1670 University Blvd, Birmingham, Alabama 35294-0019, USA*

Cardiac fibrillation (spontaneous, asynchronous contractions of cardiac muscle fibres) is the leading cause of death in the industrialized world[1], yet it is not clear how it occurs. It has been debated whether or not fibrillation is a random phenomenon. There is some determinism during fibrillation[2,3], perhaps resulting from rotating waves of electrical activity[4–6]. Here we present a new algorithm that markedly reduces the amount of data required to depict the complex spatiotemporal patterns of fibrillation. We use a potentiometric dye[7] and video imaging[8,9] to record the dynamics of transmembrane potentials at many sites during
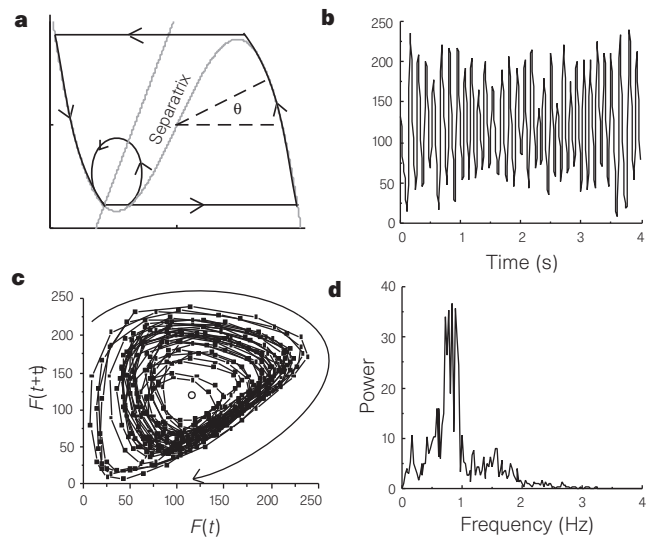

Figure 1 Temporal organization. **a**, Phase portrait of an excitable element incorporating two state variables[30]. A stable fixed point occurs at the intersection of the nullclines (dotted lines)[30]. **b**, Fluorescence signal (F) from a site on the surface of a rabbit heart during fibrillation. **c**, Phase portrait reveals trajectories circling around a centre (F_{mean}, F_{mean}), shown as a circle. **d**, The fluorescence signal exhibited a periodic component centred near 8 Hz, as observed in the corresponding power spectra. The frequency band 8 ± 3 Hz was different from equivalent white noise; $P < 0.00001$ for each heart (all sites combined).